ARTICLE | Article in Press

Planar covariation: a new key for the early detection of Duchenne muscular dystrophy walking behaviour

Ruiz Pablo · Cheron Guy · Deconinck Nicolas · Cebolla Ana Maria

Received: 24 June 2025 / Accepted: 9 October 2026
© The Author(s) 2026

Abstract

Three-dimensional gait analysis objectively quantifies lower-limb function and has been used to describe the gait pathomechanics in Duchenne muscular dystrophy (DMD) and to assess treatments. However, elevation angles, non-redundant sagittal-plane measures relative to the vertical axis, have not been examined in children with DMD, nor have gait differences between overground and treadmill walking been investigated in this population. This study investigated elevation angle profiles, planar covariation, spatiotemporal parameters, and joint kinematics in young children with DMD and typically developing (TD) children walking overground and on a treadmill. Kinematics were recorded using a Vicon motion capture system during self-selected overground and treadmill walking in twenty-five age-matched boys (fourteen with DMD; mean age 6.43 ± 1.45 years). Results showed that normalized step length and walking velocity were higher overground than on the treadmill in both groups. DMD children showed consistently wider normalized step width than TD peers. Joint kinematics did not distinguish groups across conditions, whereas elevation angles and planar covariation revealed significant overground differences in DMD children who exhibited reduced foot elevation angles bilaterally during terminal swing. They also showed smaller percent of variance on the first principal component (PV1) and larger percent of variance of the second principal component (PV2) values, with shorter, wider loops, suggesting weaker primary coordination and greater compensatory adjustments. These findings indicate that planar covariation can detect subtle gait alterations in young DMD children during overground walking, highlighting early compensatory coordination strategies not observable under treadmill pacing. Foot elevation angle modulation might serve as a sensitive marker for disease progression and treatment evaluation.

Keywords Duchenne muscular dystrophy · Planar covariation · Gait · Children · 3DGA · Treadmill · Elevation angles

This Article in Press is shared early to give you faster access to new research. It is citable and carries a permanent DOI. The final edited version will replace it automatically.

Deconinck Nicolas and Cebolla Ana Maria shared last authorship.



https://doi.org/10.1038/s41598-026-75904-3

Published online: 14 October 2026

Introduction

Duchenne muscular dystrophy (DMD) is a progressive X-linked genetic neuromuscular degenerative disorder that primarily affects male children. Progressive proximal to distal muscle weakness due to deficient expression of the dystrophin protein is a hallmark of this disease[1]. Young children with DMD develop initially subtle compensatory strategies during gait to minimize the demand on their progressively weakening muscles, which also become increasingly stiff with contractures as they age[2,3]. Motor function and ambulatory ability deteriorate over time, and walking ceases in the second decade of life. Corticosteroid treatment, a standard of care for boys with DMD, is generally initiated between 4 and 8 years of age and initially preserves strength and maintains function[4]. Novel therapeutics have been more recently developed to target genetic pathways (e.g., exon skipping, gene 'microdystrophin')[5], but unfortunately, the related clinical trials in DMD have encountered challenges in demonstrating efficacy[6,7].

In contrast to sophisticated techniques used to develop novel medications[8–11], clinical trials in neuromuscular disease typically utilize basic clinical measures such as timed and graded motor skills tests or the 6-min walk test to establish therapeutic efficacy. Current opinions from recent clinical trials suggest that these outcome measures may lack the sensitivity and specificity to detect significant improvements within the first 6–12 months of an intervention[12–15], In particular between the age of 5 and 7 where functional evaluation (for example NSAA scale) in many DMD patients does not follow a linear decline trajectory[16].

Three-dimensional gait analysis offers a method for objectively quantifying changes in lower extremity function and has been extensively used in the planning and assessment of treatments for gait pathologies[17]. The pathomechanics of gait in individuals with DMD, first described by Sutherland, et al.[18], include postural compensations of lumbar lordosis, increased anterior pelvic tilt, reduced hip extension, and increased ankle plantar flexion. Later cross-sectional studies have reported reduced peak and duration of hip extensor moments[19] and powers[20], reduced peak knee extensor moments[21], reduced plantar flexor moments[21,22], and reduced ankle power generation[20]. In addition, it has been shown that DMD boys with a history of corticosteroid exhibited greater ankle power generation during gait as compared to boys who were steroid-naïve[23] although significant differences in kinematics were absent[24].

It is important to note that nearly all findings available in the literature are based on selected temporal periods of interest rather than on analysis of the entire movement waveforms. In this line, the recent work of Vandekerckhove, et al.[25] provides a remarkable value through their detailed analysis of the entire kinematic and kinetic waveforms in their investigation for developing an up-to-date, valid DMD gait classification made by machine learning techniques using an extensive longitudinal gait database.

Gait analysis can be conducted overground or on a treadmill, presenting distinct methodological advantages and limitations. Overground walking offers a more ecological context and relies primarily on 'inside-out' motor control[26], emphasizing volitional mechanisms. However, it is often constrained by the limited size of the walking samples. In contrast, treadmill walking, a common rehabilitation tool[27,28], facilitates continuous large data acquisition but imposes an 'outside-in' motor control dynamic due to the externally driven pacing, thereby compromising ecological validity. Some biomechanical differences in spatiotemporal parameters between treadmill and overground walking in children include shorter stride length, reduced walking speed, and increased step width when children walk on a treadmill[27,29–32]. Those adaptations underscore the need to maintain stability by adopting a shorter, more frequent, and wider-based gait on the treadmill[29]. Although the differences in gait kinematics between these two walking conditions have been described in healthy children and adolescents as relatively trivial and falling within the common error range of kinematic analysis[30], they have never been explored in DMD children, even though treadmill training has been suggested for improvement in functional walking capacity and balance in children with DMD[28].

To our knowledge, among kinematic measures, no previous study has investigated elevation angles (the angle between the vertical axis (z) of the anatomical segment of interest, in the sagittal plane) measured across the

entire gait cycle in DMD. This may be because elevation angles have largely been confined to evaluating the law of intersegmental coordination, known as planar covariation[33,34] (in which a unified graphical representation of lower limb elevation angles form a loop that fits onto what it is known as the intersegmental covariation plane[33]). Nevertheless, elevation angles of lower limb segments deserve to be explored in DMD as they provide non-redundant information compared to joint angles[35]. They have been described as playing a specific role in the control of lower limb movement and as constituting a more efficient control variable than joint angles[36–38]. Besides, psychophysical evidence showed that position sense is more closely referenced to body segment elevation angles than to anatomical angles[39]. In toddlers, planar covariation is established over the first few weeks following the very first unsupported steps[40]. In addition to biomechanical constraints, planar covariation reflects not only a coordinated, centrally controlled behaviour but, interestingly, an update of the neural commands in children[40]. For this latter aspect, planar covariation might be informative of the neural commands' recalibrations accompanying the disease progression. From a practical standpoint, the regular planar loops generated by plotting elevation angles together could represent a rapid and meaningful indicator of disease-related changes.

The present study aims to investigate elevation angle profiles and planar covariation analysis, together with classical joint angle analysis, of young children with DMD and typically developing (TD) children walking in two conditions, overground and on the treadmill.

Methods

Ethics declaration

The study was approved by HUDERF Ethical Committee B4006 2020 00102; P2020/359 (pivotal study NCT04281485) and B4062024000434; P2024/630 CHU Erasme under the standards of the Declaration of Helsinki. Parents or legal tutors signed informed consent forms. All data were collected, processed, and analyzed following the current General Data Protection Regulation (RGPD) guidelines (https://gdpr—info.eu/)[41].

Participants

Twenty-five children, fourteen with DMD (14 males, 6.43 ± 1.45 years old) and eleven TD (11 males, 6.18 ± 1.60 years old) participated in the study. DMD children group's inclusion criteria were: (1) confirmed diagnosis of DMD by prior genetic testing, (2) receiving a stable daily dose of glucocorticoids for at least 3 months before enrolling and staying on daily glucocorticoids, (3) ambulatory, able to walk independently during the session. Excluded participants' criteria included: (1) recent dystrophin treatments, (2) any non-healed injury that may impact walking, and (3) any genetic abnormalities in the dystrophin gene (9, 13, 29, 30, 56–71). TD group's inclusion criteria were to be boy and age-matched with DMD peers, in good health, with no brain injury, disease, neurological, musculoskeletal, or psychiatric disorders, and absence of medication use.

Procedure and experimental protocol

The experimental sessions were conducted at the NeuroMove, Movement Neurophysiology Lab, Faculty of Human Movement Sciences, ULB, Belgium.

After a welcome and a few minutes of familiarization with the laboratory environment and providing the necessary information to both the parents and the child, the child was invited to sit comfortably to place passive motion capture markers and surface electromyographic (EMG) electrodes. Anthropometric data such as leg length (cm), body mass (kg), body height (cm), ASIS breadth (distance between anterior superior iliac spines, cm), knee diameter (cm), and malleolus width (cm) were collected. The overall quality signals were checked before the recordings started. For the first condition, the child was asked to walk at a self-selected comfortable

speed on a 4-m-long floor walkway (5 repetitions). After a break, the child was asked to redo the same condition (5 repetitions). Afterward, a safety harness (part of the laboratory's available equipment) was placed on the child to ensure safety and prevent any fall before the child was invited to stand on the treadmill. On the treadmill, the child was asked to walk at a speed he found comfortable, and the experimenter carefully adjusted the treadmill speed to similarly match the speed previously performed on the floor (5 repetitions of 10 s each). Finally, if possible, the child was asked to walk on the treadmill faster than the previously chosen (5 trials of 10 s each). Breaks were taken upon request through the experimental session. Once all conditions were completed, the child was released from the equipment, and the session was concluded after a debriefing.

Recording systems and signals

For kinematic signals, the VICON optoelectronic motion capture system was used with 10 infrared cameras working at a 100 Hz sampling rate. The retroreflective markers with adhesive stickers were attached to the participant's skin on the following anatomical landmarks, inspired by the Plug-in-gait lower limbs model (additional markers on medial epicondyles of the femur and medial ankle malleoli were placed in DMD children) a: anterior superior iliac spines (RASI-LASI), thighs (RTHI-LTHIB), medial and lateral epicondyles of the femur (RKNE-LKNE and RKNI-RKNI), shanks (RTIB-LTIB), medial and lateral ankle malleoli (RANK-LANK and RANKI-LANKI), second toes metatarsus (RTOE-LTOE), posterior superior iliac spines (RPSIP-LPSIP) and calcaneal tuberosities for heels (RHEE-LHEE).

For electromyographic signals, 14 surface EMG DELSYS wireless sensors recording at a 2000 Hz sampling rate were placed on the following muscles of both lower limbs (gluteus medius, rectus femoris, vastus lateralis, tibialis anterior, semitendinosus, gastrocnemius lateralis, and soleus). However, EMG analyses fall beyond the scope of the present study which focuses mainly on kinematic signals. The instrumented T150FMT Treadmill, Arsalis, Belgium, was used for walking on the treadmill.

Data analysis

Data were processed on NEXUS 2.1**.** Marker trajectory signals were filtered with a fourth-order Butterworth low-pass filter at 6 Hz. Gait cycles (GC) were manually detected and defined according to each lower limb's initial contact and toe-off events.

Spatiotemporal parameters were computed in Visual 3D as follows: Step length was defined as the anterior–posterior distance between contralateral heel markers at consecutive initial contacts. Step width was defined as the distance between contralateral heel markers at consecutive initial contacts in the mediolateral direction. Walking speed was calculated by dividing stride length by stride time. Cadence was defined as the number of steps per minute. These parameters were normalized according to the subject's leg length. Walking velocity was normalized by leg length and gravitational acceleration[25,42,43].

Joint Kinematics waveforms for both lower limbs (pelvis: sagittal, coronal, transversal planes; hip: sagittal, coronal, transversal planes; knee: sagittal plane; ankle: sagittal plane; foot: transversal plane) were automatically processed in Visual 3D by Cardan angles XYZ during the gait cycles:

Elevation angles: The elevation angles of the thigh, shank, and foot were calculated as the angle between the vertical axis (z) and the anatomical (thigh, shank, and foot) segment in the sagittal plane. Values were considered positive when the segment crossed anterior to the vertical axis (z) in the direction of walking (Fig. 4). The elevation angles of the thigh, shank, and foot were mean-centered. and subsequent centered elevation-angle waveforms were resampled to 101 data points per GC before being incorporated into a matrix. The matrix tracked the progression of elevation angles over time, with each column representing the elevation angle for a segment (thigh, shank, foot) and each row representing a time point.

Planar covariation: Principal Component Analysis was applied to the angle matrix. Following the covariance matrix computation, the eigenvectors (u_1, u_2, u_3, indicating the principal component's directions) and the

eigenvalues (λ_1, λ_2, λ_3, one per vector, indicating how much variance (PV, percentage of variance) is explained in each principal component (PC)) were extracted. It is well known that the first two principal components account for > 99% of the total variance in locomotion of healthy adults[33,34]; that PC1 (first principal component) captures the most variance (typically > 80%) being associated with shank and foot movement, so linked to leg coordination; that PC2 accounts for minor deviations from the principal coordination pattern described by PC1[33,44]; and that PC3 should account for only a very small proportion of the variance (PV3 < 1%), indicating that the movement remains close to a two-dimensional plane, confirming planar covariation should be very small (PV3 < 1%), indicating that the movement remains close to a plane in case the planar covariation is confirmed[33,34].

Statistics

We compared and characterized the gait of children with DMD and TD children under overground (O) and treadmill (T) walking conditions. To this end, we analyzed participant characteristics, spatiotemporal parameters, kinematic variables, planar covariation, and elevation angles.

Participant characteristics (age, body mass, and leg length) were compared between groups (DMD vs. TD) using the Mann–Whitney test due to small sample sizes, with Bonferroni correction set at $\alpha_{corr} = 0.0125$ (accounting for three individual parameters).

For gait outcomes (spatiotemporal parameters, joint kinematics, elevation angles, and planar covariation), we used permutation-based nonparametric inference implemented in Statistical (non-)Parametric Mapping (SPnM1D; vM0.4.10, https://spm1d.org/[45,46]. Specifically, we performed a permutation-based two-way mixed-design ANOVA within the SnPM1D framework, with group as the between-subject factor (DMD vs. TD), condition as the within-subject factor (T vs. O), and their interaction. Inference was conducted using 10,000 permutations whenever possible; for the within-group TD comparison (T vs. O), 2048 permutations were used due to software constraints. When significant interaction effects were observed, post hoc contrasts (T: DMD vs. TD; O: DMD vs. TD; DMD: T vs. O; TD: T vs. O) were performed using the same permutation-based approach.

Besides, to control the family-wise error rate, we applied the Bonferroni correction within each outcome family:

(1) Spatiotemporal parameters (4 variables), the significance threshold for the ANOVA main effects and interaction was set to $\alpha_{corr} = 0.0125$ (0.05/4), and the threshold for the planned post hoc comparisons (four contrasts) was set to $\alpha_{corr} = 0.0031$ (0.05/(4*4)).
(2) Joint kinematic waveforms (18 variables), the significance threshold for the ANOVA main effects and interaction was set to $\alpha_{corr} = 0.0028$ (0.05/18), and the threshold for the planned post hoc comparisons (four contrasts) was set to $\alpha_{corr} = 0.0007$ (0.05/(18*4)).
(3) Elevation-angle waveforms (6 variables), the significant threshold for the ANOVA main effects and interaction was set to $\alpha_{corr} = 0.0083$ (0.05/6), and the threshold for the planned post hoc comparisons (four contrasts) was set to $\alpha_{corr} = 0.0021$ (0.05/(6*4)).
(4) Planar covariation, for the percentage of variance (PV) explained by the three principal components in both legs (PC1, PC2, and PC3), the significant threshold for the ANOVA main effects and interaction was set to $\alpha_{corr} = 0.0083$ (0.05/6), and the threshold for the planned post hoc comparisons (four contrasts) was set to $\alpha_{corr} = 0.0021$ (0.05/(6*4)).

Results

Subject characteristics

As illustrated in Fig. 1 (Table S1, supplementary materials for more information), children had comparable ages (DMD 6.43 ± 1.45, TD 6.18 ± 1.60, $p = 0.623$), similar leg length values (DMD 54.81 ± 7.26 cm, TD 54.82 ± 7.81 cm, $p = 0.074$) and comparable body mass values (DMD 23.26 ± 4.70 kg, TD 19.77 ± 4.62 kg, $p = 0.996$).

The total mean number of GCs was 48.7 ± 26 on the treadmill (DMD 42.83 ± 27.77, TD 56.04 ± 22.01) and 13.3 ± 6.55 on the 4-m walkway (DMD 11.46 ± 6.21, TD 15.64 ± 6.36).

Spatiotemporal parameters

Concerning the spatiotemporal parameters (Fig. 2; Table S2, supplementary materials for more information), we found a significant effect of group on normalized step width (NSW) ($p = 0.0002$ between groups), where the DMD group showed wider NSW than the TD group, disregarding the condition (0.22 ± 0.04 and 0.16 ± 0.04 for DMD and TD, respectively). DMD and TD children showed smaller normalized step length (NSL) values when walking on the treadmill (0.59 ± 0.09, $p = 0.0005$ *and* 0.55 ± 0.15, $p = 0.0005$, for DMD and TD, respectively) than walking overground (0.8 ± 0.10, 0.88 ± 0.07, for DMD and TD, respectively). Normalized walking velocity (NWV) was lower in both DMD and TD children when walking on the treadmill (0.33 ± 0.05, $p = 0.0005$ *and* 0.31 ± 0.06, $p = 0.0005$, for DMD and TD, respectively) than overground (0.43 ± 0.08, 0.49 ± 0.07, for DMD and TD, respectively). Both groups preserved similar cadence in both conditions (2.31 ± 0.39 and 2.43 ± 0.30, for DMD and TD respectively, walking overground and 2.41 ± 0.30 and 2.29 ± 0.17, for DMD and TD, respectively, walking on the treadmill).

Joint kinematics

Figure 3, illustrates the initial two-way mixed ANOVA (group, DMD-TD; and conditions, O-T) results in the joint kinematics curves, for both lower limbs in sagittal, coronal, and transversal planes in DMD (pink lines for right and green lines for left lower limbs, respectively) and TD (black lines) groups during the walking overground (solid lines) and on the treadmill (dashed lines) through the entire gait cycle. The analysis showed that there were no significant differences between DMD and TD children's groups. However, significant differences in all joint kinematics curves (with the left foot progression as the unique exception) between the two conditions (Table S3, supplementary materials) were revealed: the yellow coloured bars (of variable length) embedded in the graphics of Fig. 3 represent the significant temporal clusters along the GC (discarded if shorter than 3% of GC[47]; Table S3 in supplementary materials, for precise temporal cluster limits).

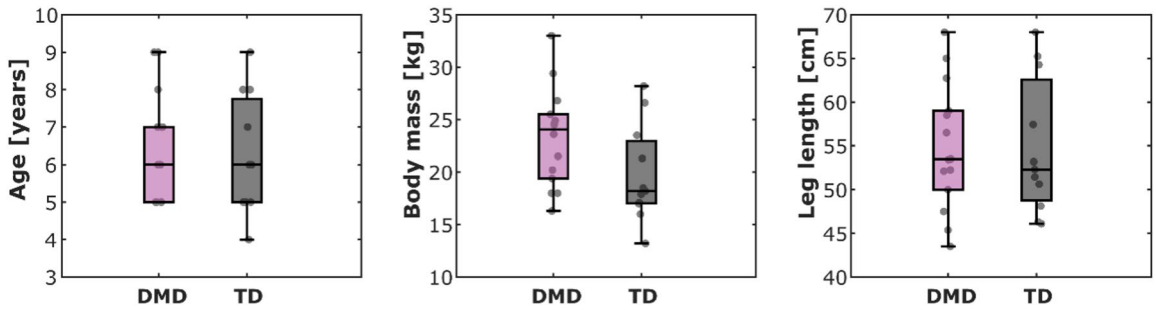

Fig. 1 Box plots of subject characteristics (age, body mass, and leg length). DMD children are represented in purple, while those of TD children are shown in grey.

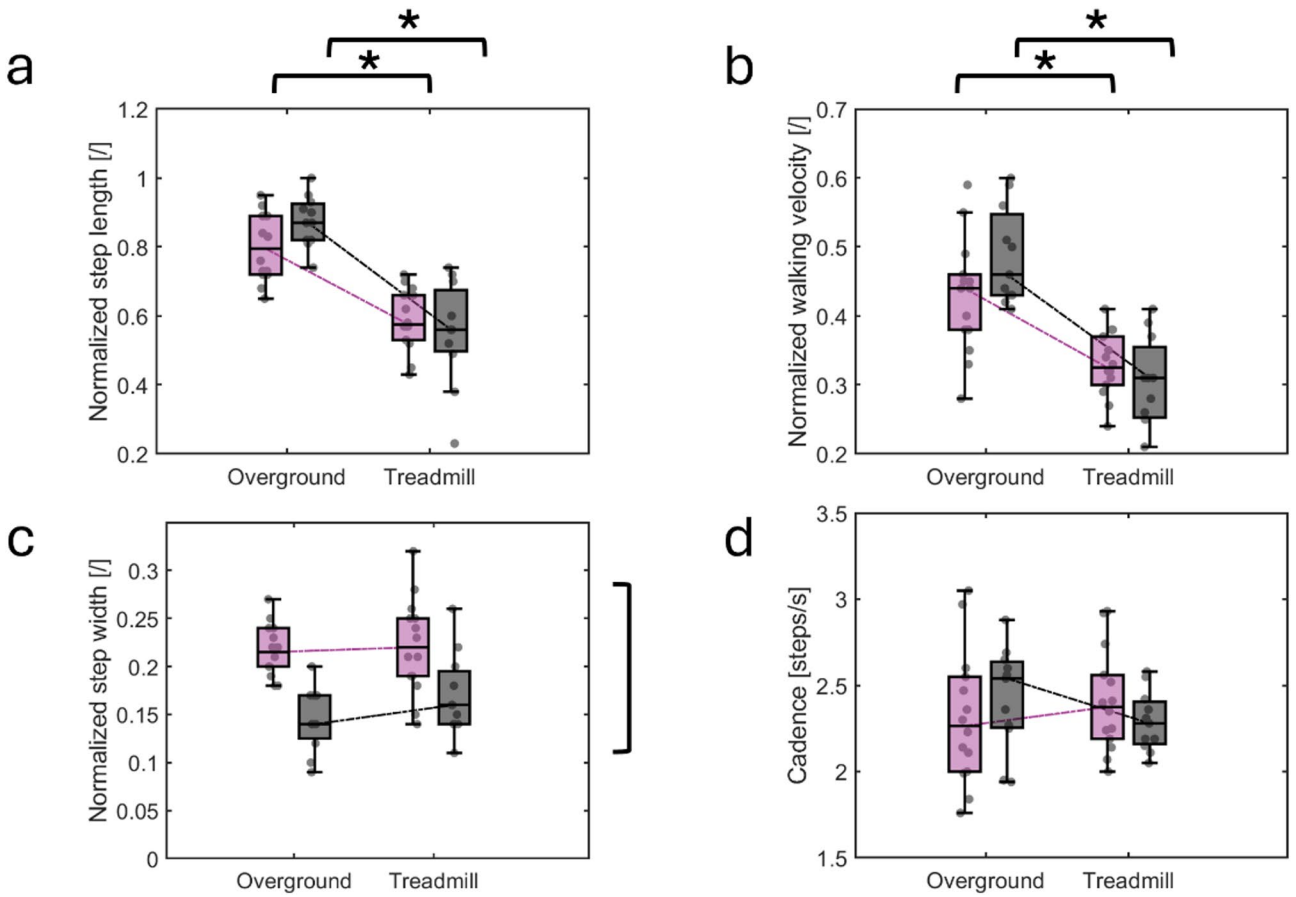

Fig. 2 Box plot of spatiotemporal parameters for overground and treadmill walking (**a**. normalized step length, **b**. normalized walking velocity, **c**. normalized step width, and **d**. cadence). Data of children with DMD are coloured in purple, while those of TD children are coloured in grey. Overground is displayed on the left, and the treadmill is on the right. The black bracket without a star indicated a significant difference in group effect (α_{corr} = 0.0125). Black stars indicate significant post hoc contrasts (α_{corr} = 0.0031).

In more detail, the groups presented the following patterns differently for walking on the treadmill than overground (Fig. 3): reduced right pelvis tilt in overground compared to treadmill walking around the loading response period (0–16%), from pre-swing to the of initial swing period (43–65%) and the terminal swing period (87–100%). The left pelvis in the sagittal plane displayed less pronounced anterior tilt values during the left toe-off event (60%) and at the end of the gait cycle (100%). Right pelvis obliquity in the coronal plane displayed lower values overground, indicating its lateral inclination in the downward direction starting from the proper heel rise (30%) event, continuing during the remaining of the stance phase (60%) and exceeding into the swing phase (70%). Left pelvis obliquity in the coronal plane displayed higher values on overground than on the treadmill from initial contact to early mid-stance phase (0 to 20%) and at the end of the GC from mid-swing and extending to the whole terminal swing 80 to 100%). Overground, the right pelvis in the transversal plane displayed more pronounced external rotation around the opposite initial contact event (50%). This latter characteristic was analogously displayed by the left pelvis, which also presented increased internal rotation overground during the loading response period (0 to 10%) and the terminal swing periods (90 to 100%). In addition, the right and left hip displayed increased extension starting from the mid-stance period (25%), occupying the terminal stance and the pre-swing periods (till 60%). Around the toe-off event (60%) and terminal swing period (90% to 100%), both right and left hips displayed more pronounced abduction. Additionally, increased external hip rotation in both legs occurred around the toe-off event and the initial contact overground. At the left and right knee joints

https://doi.org/10.1038/s41598-026-75904-3

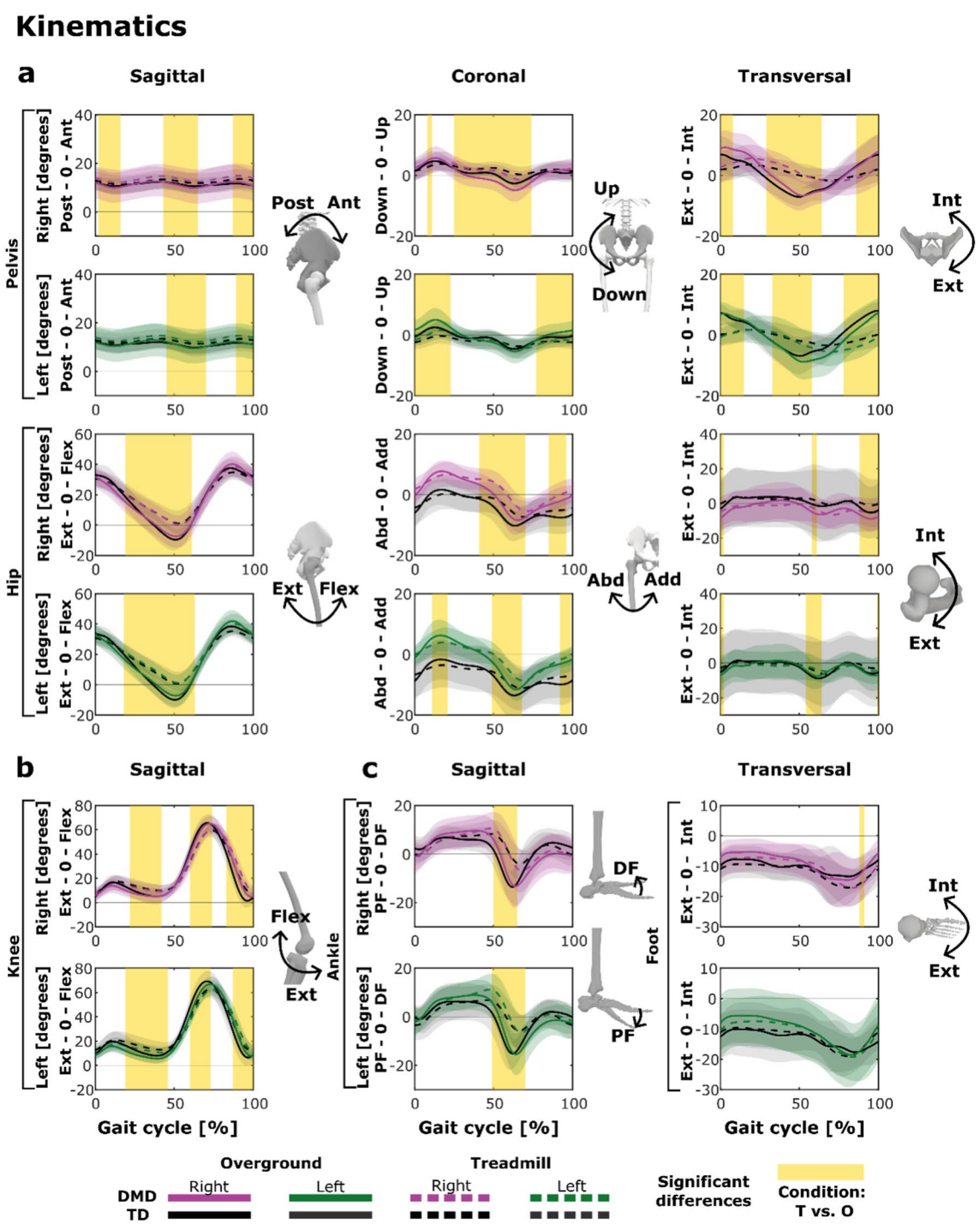

Fig. 3 Joint kinematics of DMD and TD groups are shown in both conditions (T for treadmill: dotted lines, O for overground: solid lines). The right leg (DMD in pink, TD in black) and left leg (DMD in green, TD in grey) are plotted separately. The standard deviation (SD) is indicated by shaded areas. Pelvis and hip kinematics showed in (**a**) (sagittal, coronal, and transverse plane), knee flexion–extension in (**b**), ankle dorsiflexion-plantarflexion and foot progression in (**c**). The results of the two-way mixed ANOVA by SnPM1D at α_{corr}=0.0028 are represented in the yellow area.

level, smaller flexion values were observed during the mid-stance and terminal stance periods (25% to 45%) overground, and flexion increased at the toe-off event (60%) and at the swing terminal periods (87% to 100%) Finally, at ankle level, increased plantar flexion in both legs around toe-off event (60%), and increased external foot progression only in right foot in the beginning of terminal swing (87%).

Elevation angles

Figure 4 illustrates the foot, shank, and thigh elevation angles during the gait cycle for the DMD (in pink and green lines for right and left lower limbs, respectively) and TD children (in black lines) during their walking on the treadmill (dotted lines) and overground (continuous lines). The significant differences (α_{corr}=0.0083) in group effect (DMD and TD groups) are indicated by vertical, blue light-coloured bars, indicating the significant temporal clusters along the gait cycle (Table S4 in supplementary material for precise values).

Significant differences were observed in condition effect (Overground and Treadmill conditions, yellow-coloured vertical bars, Table S5 in supplementary material for precise values); such changes occurred during the same three gait cycle temporal slots: (1) at the initial contact during the loading response period; (2) around the opposite initial contact event (50%) during the terminal stance and pre-swing before the toe-off event at 60%; and (3) during the terminal swing (90–100%). The three elevation angles were bigger walking overground for both the right and left sides than on the treadmill.

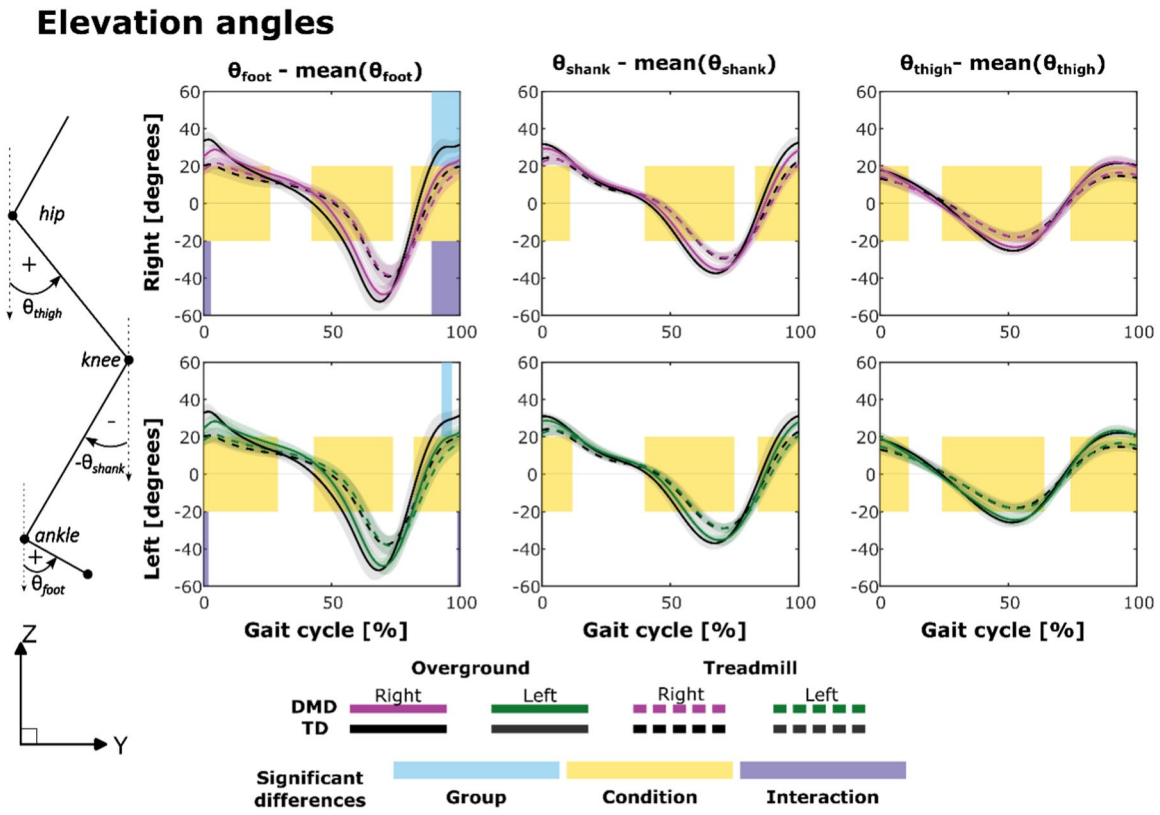

Fig. 4 The mean-centered elevation angles of the DMD and TD groups are displayed with solid lines for the overground condition and dotted lines for the treadmill. The right leg (DMD in purple, TD in black) and left leg (DMD in green, TD in grey) are plotted separately. The standard deviation (SD) is indicated by shaded areas. The results of the two-way mixed ANOVA by SnPM1D at α_{corr}=0.0083 are represented in the light blue (group), yellow (condition), and purple (group × condition interaction) areas.

For the group effects, both DMD and TD children groups showed similar patterns of elevation angles across all walking conditions, except during the terminal swing period (around 90% to 100%) preceding the next initial contact event during overground walking, and only for foot elevation.

Significant differences in the interaction effect (group × condition, illustrated in purple vertical bars) occurred only in the mean-centered foot elevation angle, in the terminal swing and the next initial contact (Table S6 in the supplementary material for precise values). Subsequent post hoc contrasts (α_{corr}=0.0021) for DMD: O vs. T and for TD: O vs. T, showed significant differences around the terminal swing and the next initial contact (Tables S7 and S8 in the supplementary material for precise values). In addition, post hoc contrast for T: DMD vs. TD did not show significant differences. Finally, the post hoc contrast for O: DMD vs. TD revealed significant differences (described below with the planar covariation analysis and illustrated in Fig. 6).

Planar covariation

The mean loops of planar covariation correspond to the time-dependent evolution of the elevation angles (thigh, shank, and foot) in a 3D space throughout the locomotion cycle. It is important to note that the loops do not provide temporal precision but a unified configuration evolution of the three segments. Figure 5a illustrates the mean loops of planar covariation of the right and left inferior limb segments (pink and green coloured loops, respectively) for overground (on the left) and, on the treadmill (on the right) walking types, for DMD and TD children's groups.

These graphical representations (Fig. 5a) allowed an immediate visual identification of a shorter and wider loop in children with DMD compared to TD children during overground walking.

Figure 5b includes the percentage of variance (PV) box plots per component, for the right lower limb (Fig. 5b.1, in purple and black colours for DMD and TD children's groups, respectively) and for the left lower limb (Fig. 5b.2, in green and black colours for DMD and TD children's groups, respectively). The analysis showed that PV3 remained always below 1%, confirming planar covariation for locomotion in both groups and for both types of walking. The analysis also revealed significant differences between conditions, disregarding the group, in PV1 and PV2 of the right leg, with higher PV1 (85.8±3.32 O, 83.6±3.58 T) and lower PV2 (13.7±3.42 O, 15.7±3.65 T; $p=0.0002$ for PV1, $p=0.0004$ for PV2). In the left leg, DMD children showed smaller PV1 and higher PV2 values than TD children, disregarding the conditions (PV1 82.7±3.17 in DMD versus 86±3 in TD, $p=0.006$, and PV2 16.8±3.17 in DMD versus 13.4±2.96 in TD, $p=0.005$).

These differences between PV1 and PV2 between the groups, lead to the observed shorter and wider loop for the left lower limb in DMD children as illustrated in Fig. 5a (Table S10 in supplementary material for precise values).

Figure 6a reproduces the mean loops of planar covariation for both groups walking overground, and Fig. 6b the related results of the post hoc contrast ((α_{corr}=0.0021) O: DMD vs. TD). Note that the statistical differences are highlighted now in the related part of the loop corresponding to the terminal swing period for the foot elevation angle (around 90%). In addition, Fig. 6c illustrates the corresponding foot elevation angle curves (previously analysed in Fig. 4) in the post-hoc contrast, DMD vs. TD overground (α_{corr}=0.0021). In this representation, we have used a lagged gait cycle (starting at the toe off event) to emphasize the significant cluster during the terminal swing period and next initial contact. At this moment, DMD children had lower foot elevation angles than the TD group (Table S9 in supplementary material for precise values).

Discussion

To our knowledge, this is the first study to investigate elevation angle profiles and planar covariation analysis, together with classical joint angle analysis, in young children with DMD and typically developing (TD) children walking both overground and on a treadmill.

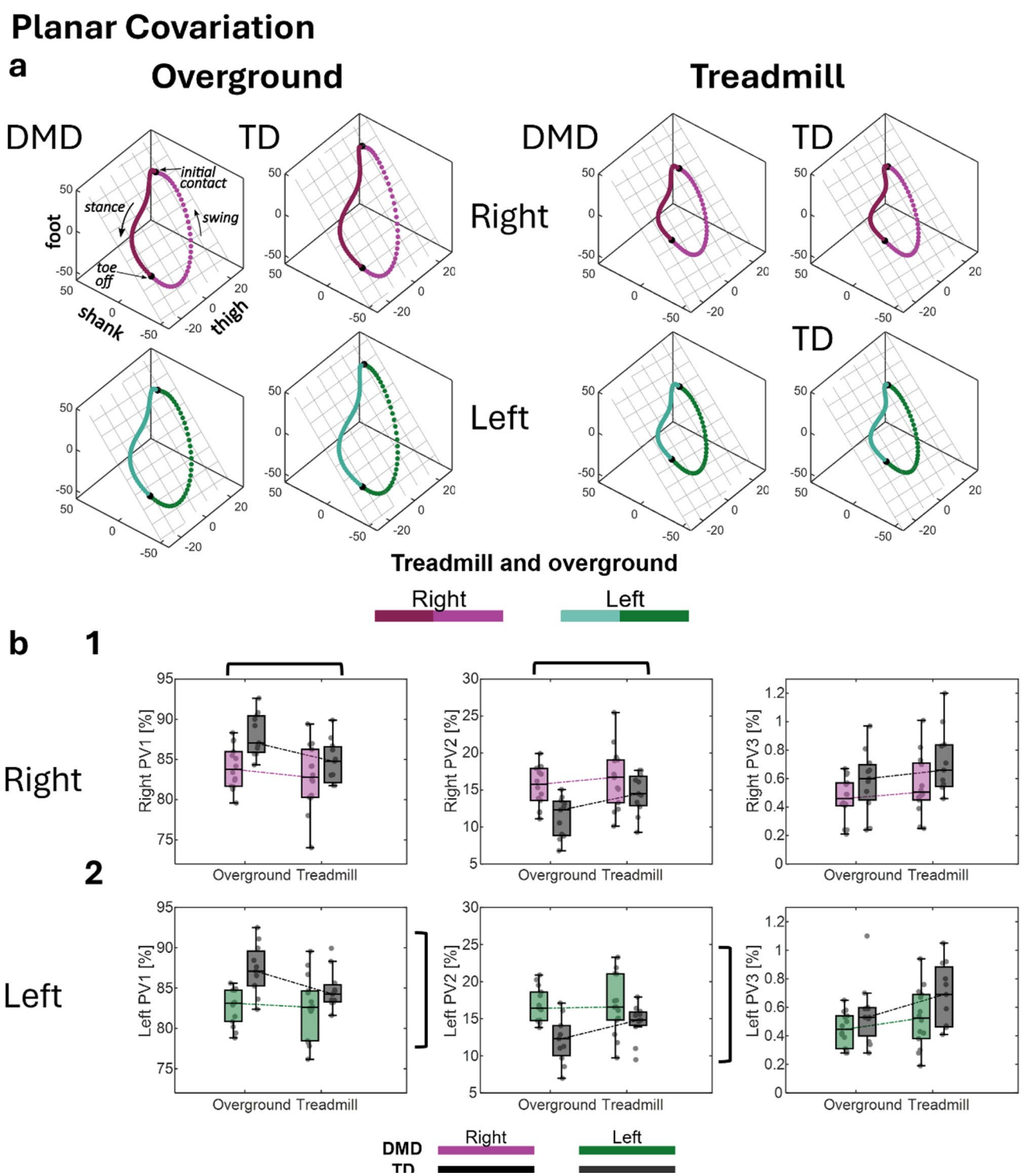

Fig. 5 Planar covariation loops (**a**) and percentage of variance (PV) (**b**). Box plots (5b.1 and 5b.2) are shown for groups (DMD in pink and green for right and left lower limbs, respectively; and TD children in black) and walking conditions (Overground and Treadmill). The results of the two-way mixed ANOVA by SnPM1D at α_{corr}=0.0083 are represented by brackets for the main effects of group and condition (vertical and horizontal, respectively).

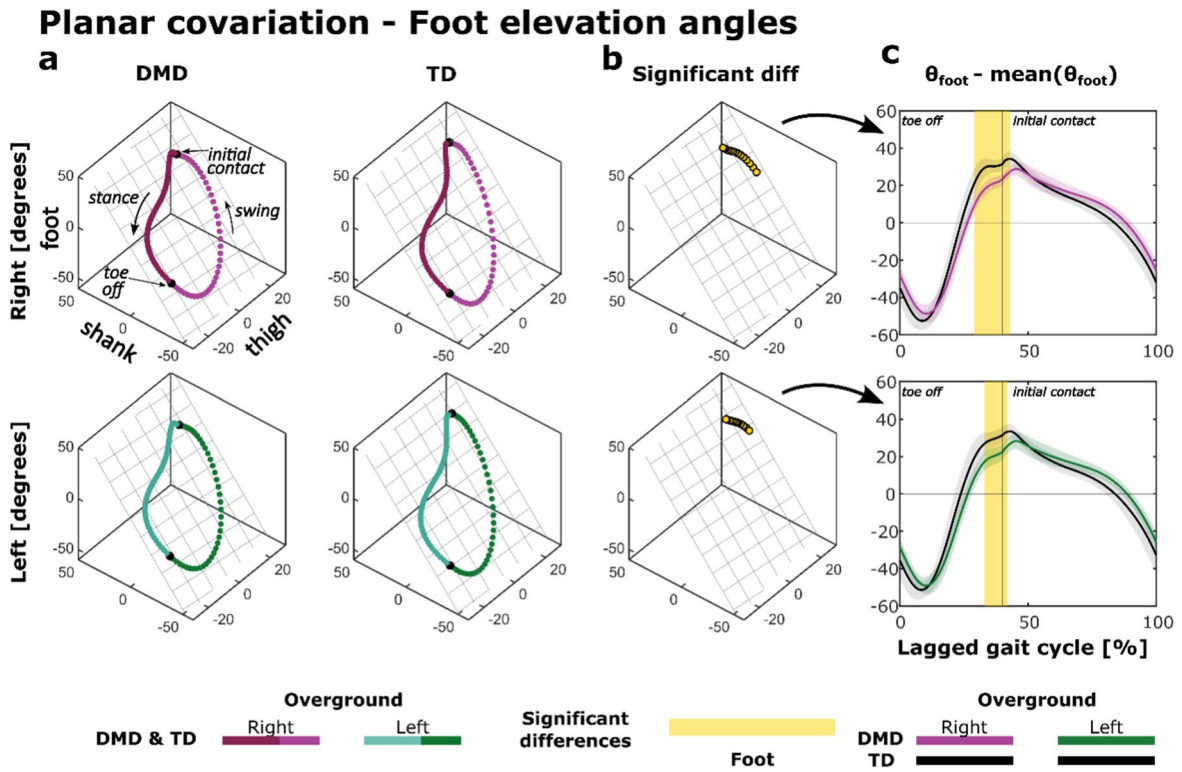

Fig. 6 Planar covariation loops of foot shank and thigh elevation angles in pink and green for right and left side, respectively (**a**); the results of the post hoc contrast (α_{corr}=0.0021) DMD vs. TD, overground (in yellow) (**b**); the mean-centered foot elevation angles (**c**) when the DMD and TD groups walk overground (significant differences in the yellow area).

The spatiotemporal parameters indicated that walking on the treadmill did not pose any additional difficulty to the DMD compared to the TD group, and both groups of children showed shorter normalized step length and smaller normalized walking velocity on the treadmill, in agreement with previous studies with TD children[27,29,32,48]. Our DMD children's group presented distinctive normalized step width, being wider than the TD group regardless the condition, as previously described for older DMD children[49]. This finding corroborates the proposition of the increase of step width as an index of reduced stability accounting for the quality of locomotion[50]. Although cadence seemed to follow different patterns in DMD and TD children, the differences were not statistically significant. As Dal, et al.[51] explained, the decrease in cadence on the treadmill could be related to the decrease in speed compared to overground walking in TD children.

Regarding classical joint kinematics, we did not find group differences, and both groups showed adaptations at all joint levels, in all planes, and on both sides (pelvis, hip, knee, and ankle; sagittal, coronal, and transverse planes; right and left); overall, joint ranges of motion were reduced during treadmill walking compared with overground walking[27,30,32].

It is important to note that the children participating in our study were younger (around 6.4 years old) than those in previous studies[19,25,49,52], corresponding to an early stage of the disease (Sutherland, et al.[18]). It has been previously described that at this early stage the spatiotemporal parameters and the kinematics differences appear too subtle to be easily detected. They may include an increased cadence, a step length decrease, an increased anterior–posterior pelvic tilt and pelvic rotation ranges, an increased plantarflexion during the swing phase, and a decreased maximum dorsiflexion at the ankle[21]. As the degenerative disease progresses from the early to the transitional stage (around 8.3 years old)[18], the pathomechanics of gait in DMD feature a decreased cadence and velocity[53]; an increased pelvic tilt with decreased maximal hip extension and hip flexion in stance and swing

phases, respectively; a decreased maximum of ankle dorsiflexion in the swing phase; and an increased maximum foot internal rotation in the stance phase[18].

In a systematic review[24], the analysis of seventy-nine spatiotemporal, kinematic, kinetic, and muscular activity parameters in children with DMD, showed that decreased walking speed, decreased stride length, and decreased step length were the most consistently reported features. It was also shown that kinematics of the knee presented an increased range of motion, while the ankle joint exhibited a lower maximum dorsiflexion angle during the swing phase. Regarding kinetics, the hip showed a lower maximum extension torque during stance (10–15%) and reduced maximum power generation during propulsion (45–55%). Similarly, the ankle presented a lower maximum dorsiflexion torque at weight acceptance (10–15%) and decreased maximum power generation during push-off.

Based on the previously described joint kinematic patterns, our DMD group could belong to the Mildly Group presented by Vandekerckhove, et al.[25], despite a lower step width in our DMD group, and individual characteristics differences (our children with DMD were younger, with shorter leg length).

It seems reasonable to hypothesize that walking on the treadmill could have exposed kinematics distinctions between both groups of children because of the possible inherent challenges to balance imposed by the treadmill[31] or the motor learning challenge to control the movement[54] including the visual-motor mismatch[48]. However, both groups of children achieved similarly. It can be suggested that walking on the treadmill imposes mechanical interactions and visual information restrictions that could force the ubiquity emergence of the invariant characteristics of the kinematics by the motor systems[55].

Interestingly, despite the young age of the participants (DMD 6.43 ± 1.45, TD 6.18 ± 1.60), elevation angles and planar covariation analyses detected significant differences between groups for overground walking, whereas kinematic joints were not significantly distinctive. Concretely, during the terminal swing period and at the next initial contact (around 90% to 100%), DMD children presented smaller values for the right and left foot elevation angles than the TD group. Subsequent planar covariation analysis revealed that DMD children showed smaller PV1 and higher PV2 values than TD children, what lead to shorter and wider-shaped loop in children with DMD overground.

Differences in PV1 and PV2 have been previously described between healthy children of 5 and 10 years when walking overground at 3 km/h[56]. Interestingly, our DMD children exhibited lower PV1 and higher PV2, like the 5-year children group, while our TD children maintained higher PV1 and lower PV2, like the 10-year-old children group. This might suggest that DMD children have not yet achieved a mature pattern like their TD peers[40]. As PV1 accounts for a primary coordination pattern, lower PV1 in our children with DMD could suggest less adaptability in their main joint coordination pattern. In the same line, PV2 accounting for additional variance beyond the primary coordination pattern of PV1, it reflects secondary modulations of intersegmental coordination[33,44]. Thus, higher PV2 in our DMD group could reflect stronger adjustment requirements. These adjustments may correspond to the reduced range of motion observed in the foot-elevation angle around initial contact in children with DMD walking overground. This could be explained by dorsiflexion weakness and plantarflexion contractures, as suggested by Vandekerckhove, et al.[57].

Kinematics joints and elevation angles provide non-redundant information, and there is no simple geometrical transformation between anatomical and elevation angles[35]. It has been proposed that planar covariation may reflect a coordinated, central behavior[58] to control the orientation of limb segments, and that it can be elicited or repressed by sensorimotor cues[59]. In this way, the central nervous system would have two possible options depending on the sets of variables it controls, either kinematic joints or elevation angles[35]: For kinematic joints control, proprioceptive information would be the major input, as no external information is required to detect relative angles. In contrast, for elevation angles control, both proprioceptive and exteroceptive information would be relevant inputs, as external cues are essential for determining the direction of gravity[60]. Accordingly, we could hypothesize that the significant elevation angles change, clearly featured by a shorter and wider-shaped loop, for the overground walking in DMD children with respect to TD children's groups. It may reflect exteroceptive more than proprioceptive information integration distinction in controlling foot elevation angles. Furthermore, the lack

of significant differences (nor in joint kinematics nor elevation angles), between DMD and TD children's group during their walking on the treadmill, could be interpreted as if this walking type would impose a sensory (visual, touch, vestibular, even auditory) information weighting reduction, thus becoming not relevant for the distinction. On the contrary, overground walking would imply a heavier weight of multimodal sensory information integration through their reafferences. Moreover, the overground walking type could be interpreted as a less predictable environment than the treadmill one by the brain "from inside out", under Buzsáki's view as a foretelling device that interacts with environments through action and examination of action's consequences[26].

The planar law of intersegmental coordination is not a simple consequence of biomechanics[58,61], and good evidence supports its functional value in the control of locomotion[62], during which it would emerge from the interaction between spinal neural networks and limb mechanical oscillators[59]. In this line, phase-adjusted sinusoidal signals extracted from elevation angles can describe the characteristics of planar covariation[35] and more, a fully connected recurrent neural network can reproduce human walking patterns of lower limb elevation angles from simple oscillations corresponding to the harmonics of such kinematics[63]. Besides, the study of lower-limb elevation angles has provided insight into the neurophysiological mechanisms underlying human gait coordination, explaining both its energy efficiency[33,34,64] and its capacity for anticipation and adaptation[37].

Dewolf, et al.[65] have shown by means of the planar covariation that elderly adults presented a specific alteration of the foot-shank coordination, indicating that this feature involves a complex coordination highly dependent on the maintenance of neuro-biomechanical factors. Amongst those, the slowing of motor and sensory conduction velocity[66,67], the loss of tactile acuity[68], and the sense of joint position[69] may complicate the effects of a weaker force resulting in motor strategy adaptation[70]. Such type of sensorimotor adaptation might explain the present alteration in the foot-shank coordination in DMD children.

Recently, Nunez-Lisboa, et al.[71] showed that voluntary trunk inclination during walking induces a modification of the anticipatory phase of heel strike, thereby demonstrating the existence of whole-body coordination around the gravitational axis. The initial contact represents a crucial stage in gait control[33,34,37]. In typical gait, the heel makes the first contact with the ground[72–74], a pattern that promotes efficient and economical walking[75]; however, this requires adequate foot elevation during the swing phase prior to heel strike. Our children with DMD exhibited smaller foot elevation angles prior to the next initial contact: we speculate that this specific foot elevation command results from a peculiar computation considering the integration of the vertical body posture and the predictive forward position of the foot at the crucial moment of initial contact on the ground.

The diminished foot angle elevation observed in DMD, could result from multiple neuronal deficits linked to GABAergic modulation originating in cortical and cerebellar systems, which converge into central pattern generators (CPGs)[76] networks. From a translational perspective, the absence of dystrophin in mdx mice disrupts postsynaptic GABAA receptor clustering, reducing inhibitory input to cerebellar Purkinje cells[77,78]. This is associated with altered Purkinje cell firing and fast (160–200 Hz) LFP oscillations in awake mdx mice[79]. Structural changes in the corticospinal system have also been reported[80,81]. Dystrophin and its associated protein complex stabilize postsynaptic GABAA receptors by regulating peri- and extrasynaptic trafficking[82]. Given the presence of GABAA receptors[83,84] and dystrophin[85,86] in the spinal cord, this mechanism[82] may contribute to the fine regulation of central pattern generators and motoneuronal output.

This study has several limitations. Although early childhood represents a clinically relevant period in Duchenne muscular dystrophy (DMD), as corticosteroid therapy is typically initiated between 4 and 8 years of age and emerging genetic therapies increasingly target young children, the inclusion of participants under six years likely introduced age-related variability, given that gait and joint kinematics are still maturing. While visual inspection (Figs. 3 and 4) suggests that the standard deviation of elevation angles may be smaller than that of joint angles and comparable between groups, this observation remains qualitative and requires confirmation. Moreover, the small sample size in both groups limits statistical power and restricts the generalizability of our findings.

Further investigation involving longitudinal studies with a larger number of participants is needed to confirm the relevance of elevation angles and planar covariation in the early detection of gait changes in DMD, tracking the progression of the disorder, and possibly evaluating the efficacy of medical treatments such as gene therapy.

Although muscle weakness is a major hallmark in DMD, further research is also needed to understand the physiological mechanisms of patho-clinics mechanisms[24]. In this line, complementing planar covariation analysis with the study of muscle activity using surface electromyography might provide future deeper insights into children's coordination strategies and compensations while walking in various environments.

Conclusion

Our findings suggest that planar covariation can detect subtle changes in the overground locomotion of young children with DMD compared to TD. This finding highlights the emergence of a compensatory gait coordination strategy in children with DMD, specifically involving volitional control mechanisms that are not observable under externally paced treadmill conditions at this early age.

The modulation of foot elevation angle under these conditions might serve as a sensitive biomechanical marker for tracking disease progression and evaluating the efficacy of emerging therapeutic interventions in Duchenne muscular dystrophy.

Supplementary Information The online version contains supplementary material available at https://doi.org/10.1038/s41598-026-75904-3.

Acknowledgements We thank the Belgian Kids' Fund for Pediatric Research and the Duchenne Parent Project Belgium for their support. We are grateful to Mathieu Petieau and Jean-Paul Kaleeta for their assistance with data collection.

Author contributions Conceptualization: ND, AMC, GC. Data curation: PR, AMC. Formal analysis: PR, AMC, GC. Funding acquisition: ND, AMC. Investigation: PR. Methodology: AMC, PR. Project administration: AMC et ND. Resources: AMC et ND. Software: PR. Supervision: AMC, ND, GC. Validation: AMC, GC, ND. Visualization: PR. Writing original draft: PR, AMC. Writing- review & editing: PR, GC, ND, AMC.

Funding This work was supported by a grant from The Belgian Kids' Fund for Pediatric Research, awarded to P.R.

Data availability Data are available upon request from the corresponding author, A.M.C.

Declarations

Competing interests The authors declare no competing interests.

Open Access This article is licensed under a Creative Commons Attribution-NonCommercial-NoDerivatives 4.0 International License, which permits any non-commercial use, sharing, distribution and reproduction in any medium or format, as long as you give appropriate credit to the original author(s) and the source, provide a link to the Creative Commons licence, and indicate if you modified the licensed material. You do not have permission under this licence to share adapted material derived from this article or parts of it. The images or other third party material in this article are included in the article's Creative Commons licence, unless indicated otherwise in a credit line to the material. If material is not included in the article's Creative Commons licence and your intended use is not permitted by statutory regulation or exceeds the permitted use, you will need to obtain permission directly from the copyright holder. To view a copy of this licence, visit http://creativecommons.org/licenses/by-nc-nd/4.0/.

References

1. Hoffman, E. P. et al. Restoring dystrophin expression in Duchenne muscular dystrophy muscle progress in exon skipping and stop codon read through. *Am. J. Pathol.* **179**, 12–22. https://doi.org/10.1016/j.ajpath.2011.03.050 (2011).
2. Deconinck, N. & Dan, B. Pathophysiology of Duchenne muscular dystrophy: Current hypotheses. *Pediatr. Neurol.* **36**, 1–7. https://doi.org/10.1016/j.pediatrneurol.2006.09.016 (2007).
3. Duan, D., Goemans, N., Takeda, S., Mercuri, E. & Aartsma-Rus, A. Duchenne muscular dystrophy. *Nat. Rev. Dis. Primers* **7**, 13. https://doi.org/10.1038/s41572-021-00248-3 (2021).

4. Bushby, K. et al. Diagnosis and management of Duchenne muscular dystrophy, part 1: Diagnosis, and pharmacological and psychosocial management. *Lancet Neurol.* **9**, 77–93. https://doi.org/10.1016/S1474-4422(09)70271-6 (2010).
5. Duan, D. Systemic AAV micro-dystrophin gene therapy for Duchenne muscular dystrophy. *Mol. Ther.* **26**, 2337–2356. https://doi.org/10.1016/j.ymthe.2018.07.011 (2018).
6. Scully, M. A., Pandya, S. & Moxley, R. T. Review of Phase II and Phase III clinical trials for Duchenne muscular dystrophy. *Expert Opin. Orphan Drugs* **1**, 33–46. https://doi.org/10.1517/21678707.2013.746939 (2012).
7. Merlini, L. & Sabatelli, P. Improving clinical trial design for Duchenne muscular dystrophy. *BMC Neurol.* https://doi.org/10.1186/s12883-015-0408-z (2015).
8. Kornegay, J. N. et al. Pharmacologic management of Duchenne muscular dystrophy: Target identification and preclinical trials. *ILAR J.* **55**, 119–149. https://doi.org/10.1093/ilar/ilu011 (2014).
9. Henricson, E. K. et al. The cooperative international neuromuscular research group Duchenne natural history study: Glucocorticoid treatment preserves clinically meaningful functional milestones and reduces rate of disease progression as measured by manual muscle testing and other commonly used clinical trial outcome measures. *Muscle Nerve* **48**, 55–67. https://doi.org/10.1002/mus.23808 (2013).
10. Lynn, S. et al. Measuring clinical effectiveness of medicinal products for the treatment of Duchenne muscular dystrophy. *Neuromuscul. Disord.* **25**, 96–105. https://doi.org/10.1016/j.nmd.2014.09.003 (2015).
11. Kirschner, J. et al. Treatment of Duchenne muscular dystrophy with ciclosporin A: A randomised, double-blind, placebo-controlled multicentre trial. *Lancet Neurol.* **9**, 1053–1059. https://doi.org/10.1016/S1474-4422(10)70196-4 (2010).
12. Lu, Q. L., Cirak, S. & Partridge, T. What can we learn from clinical trials of exon skipping for DMD?. *Mol. Ther. Nucleic Acids* **3**, e152. https://doi.org/10.1038/mtna.2014.6 (2014).
13. Haas, M. et al. European Medicines Agency review of ataluren for the treatment of ambulant patients aged 5 years and older with Duchenne muscular dystrophy resulting from a nonsense mutation in the dystrophin gene. *Neuromuscul. Disord.* **25**, 5–13. https://doi.org/10.1016/j.nmd.2014.11.011 (2015).
14. McDonald, C. M. et al. The 6-minute walk test as a new outcome measure in Duchenne muscular dystrophy. *Muscle Nerve* **41**, 500–510. https://doi.org/10.1002/mus.21544 (2010).
15. Scott, E. et al. Development of a functional assessment scale for ambulatory boys with Duchenne muscular dystrophy. *Physiother. Res. Int.* **17**, 101–109. https://doi.org/10.1002/pri.520 (2012).
16. Goemans, N. et al. Suitability of external controls for drug evaluation in Duchenne muscular dystrophy. *Neurology* **95**, e1381–e1391. https://doi.org/10.1212/WNL.0000000000010170 (2020).
17. Wren, T. A., Gorton, G. E. 3rd., Ounpuu, S. & Tucker, C. A. Efficacy of clinical gait analysis: A systematic review. *Gait Posture* **34**, 149–153. https://doi.org/10.1016/j.gaitpost.2011.03.027 (2011).
18. Sutherland, D. H. et al. The pathomechanics of gait in Duchenne muscular dystrophy. *Dev. Med. Child Neurol.* **23**, 3–22. https://doi.org/10.1111/j.1469-8749.1981.tb08442.x (1981).
19. Gaudreault, N., Gravel, D., Nadeau, S., Houde, S. & Gagnon, D. Gait patterns comparison of children with Duchenne muscular dystrophy to those of control subjects considering the effect of gait velocity. *Gait Posture* **32**, 342–347. https://doi.org/10.1016/j.gaitpost.2010.06.003 (2010).
20. D'Angelo, M. G. et al. Gait pattern in Duchenne muscular dystrophy. *Gait Posture* **29**, 36–41. https://doi.org/10.1016/j.gaitpost.2008.06.002 (2009).
21. Doglio, L. et al. Early signs of gait deviation in Duchenne muscular dystrophy. *Eur. J. Phys. Rehabil. Med.* **47**, 587–594 (2011).
22. Sienko, S. et al. Kinematic changes in gait in boys with Duchenne muscular dystrophy: Utility of the gait deviation index, the gait profile score and the gait variable scores. *Gait Posture* **100**, 157–164. https://doi.org/10.1016/j.gaitpost.2022.12.007 (2023).
23. Heberer, K. et al. Hip kinetics during gait are clinically meaningful outcomes in young boys with Duchenne muscular dystrophy. *Gait Posture* **48**, 159–164. https://doi.org/10.1016/j.gaitpost.2016.05.013 (2016).
24. Goudriaan, M. et al. Gait deviations in Duchenne muscular dystrophy-Part 1. A systematic review. *Gait Posture* **62**, 247–261. https://doi.org/10.1016/j.gaitpost.2018.03.020 (2018).
25. Vandekerckhove, I. et al. Gait classification for growing children with Duchenne muscular dystrophy. *Sci. Rep.* **14**, 10828. https://doi.org/10.1038/s41598-024-61231-y (2024).
26. Buzsáki, G. M. *The Brain from Inside Out* (Oxford University Press, 2019).
27. Mace, S. N., Harrington, J. W., Knarr, B. A. & Kingston, D. C. Overground, conventional treadmill, and aquatic treadmill walking joint kinematics differ in typically developing children and adolescents. *J. Biomech.* **188**, 112764. https://doi.org/10.1016/j.jbiomech.2025.112764 (2025).
28. Sherief, A., Abd ElAziz, H. G. & Ali, M. S. Efficacy of two intervention approaches on functional walking capacity and balance in children with Duchene muscular dystrophy. *J. Musculoskelet. Neuronal Interact.* **21**, 343–350 (2021).
29. Stolze, H. et al. Gait analysis during treadmill and overground locomotion in children and adults. *Electroencephalogr. Clin. Neurophysiol.* **105**, 490–497. https://doi.org/10.1016/s0924-980x(97)00055-6 (1997).
30. Jung, T. et al. Comparison of treadmill and overground walking in children and adolescents. *Percept. Mot. Skills* **128**, 988–1001. https://doi.org/10.1177/0031512521993102 (2021).

31. Semaan, M. B. et al. Is treadmill walking biomechanically comparable to overground walking? A systematic review. *Gait Posture* **92**, 249–257. https://doi.org/10.1016/j.gaitpost.2021.11.009 (2022).
32. Senden, R. et al. Comparison of sagittal plane gait characteristics between the overground and treadmill approach for gait analysis in typically developing children. *PeerJ* **10**, e13752. https://doi.org/10.7717/peerj.13752 (2022).
33. Borghese, N. A., Bianchi, L. & Lacquaniti, F. Kinematic determinants of human locomotion. *J. Physiol.* **494**(Pt 3), 863–879. https://doi.org/10.1113/jphysiol.1996.sp021539 (1996).
34. Bianchi, L., Angelini, D. & Lacquaniti, F. Individual characteristics of human walking mechanics. *Pflugers Arch.* **436**, 343–356. https://doi.org/10.1007/s004240050642 (1998).
35. Barliya, A., Omlor, L., Giese, M. A. & Flash, T. An analytical formulation of the law of intersegmental coordination during human locomotion. *Exp. Brain Res.* **193**, 371–385. https://doi.org/10.1007/s00221-008-1633-0 (2009).
36. Israeli-Korn, S. D. et al. Intersegmental coordination patterns are differently affected in Parkinson's disease and cerebellar ataxia. *J. Neurophysiol.* **121**, 672–689. https://doi.org/10.1152/jn.00788.2017 (2019).
37. Leurs, F. et al. Planar covariation of elevation angles in prosthetic gait. *Gait Posture* **35**, 647–652. https://doi.org/10.1016/j.gaitpost.2011.12.017 (2012).
38. Courtine, G. & Schieppati, M. Tuning of a basic coordination pattern constructs straight-ahead and curved walking in humans. *J. Neurophysiol.* **91**, 1524–1535. https://doi.org/10.1152/jn.00817.2003 (2004).
39. Soechting, J. F. & Ross, B. Psychophysical determination of coordinate representation of human arm orientation. *Neuroscience* **13**, 595–604. https://doi.org/10.1016/0306-4522(84)90252-5 (1984).
40. Cheron, G. et al. Development of a kinematic coordination pattern in toddler locomotion: Planar covariation. *Exp. Brain Res.* **137**, 455–466. https://doi.org/10.1007/s002210000663 (2001).
41. European, P. & Council of the European, U. In *Official Journal of the European Union* Vol. 119 1–88 (2016).
42. Hof, A. L. Scaling gait data to body size. *Gait Posture* **4**, 222–223. https://doi.org/10.1016/0966-6362(95)01057-2 (1996).
43. Stansfield, B. W. et al. Normalisation of gait data in children. *Gait Posture* **17**, 81–87. https://doi.org/10.1016/s0966-6362(02)00062-0 (2003).
44. Lacquaniti, F., Ivanenko, Y. P. & Zago, M. Kinematic control of walking. *Arch. Ital. Biol.* **140**, 263–272 (2002).
45. Nichols, T. E. & Holmes, A. P. Nonparametric permutation tests for functional neuroimaging: A primer with examples. *Hum. Brain Mapp.* **15**, 1–25. https://doi.org/10.1002/hbm.1058 (2002).
46. Pataky, T. C., Vanrenterghem, J. & Robinson, M. A. The probability of false positives in zero-dimensional analyses of one-dimensional kinematic, force and EMG trajectories. *J. Biomech.* **49**, 1468–1476. https://doi.org/10.1016/j.jbiomech.2016.03.032 (2016).
47. Kainz, H. et al. Reliability of four models for clinical gait analysis. *Gait Posture* **54**, 325–331 (2017).
48. Tesio, L. et al. Gait analysis on force treadmill in children: Comparison with results from ground-based force platforms. *Int. J. Rehabil. Res.* **40**, 315–324. https://doi.org/10.1097/MRR.0000000000000243 (2017).
49. Romkes, J., Bracht-Schweizer, K., Widmer, M., Sangeux, M. & Viehweger, E. Upper body gait deviations in children with Duchenne muscular dystrophy. *Clin. Biomech.* **122**, 106402. https://doi.org/10.1016/j.clinbiomech.2024.106402 (2025).
50. Romano, A. et al. Evaluation of gait in Duchenne muscular dystrophy: Relation of 3D gait analysis to clinical assessment. *Neuromuscul. Disord.* **29**, 920–929. https://doi.org/10.1016/j.nmd.2019.10.007 (2019).
51. Dal, U., Erdogan, T., Resitoglu, B. & Beydagi, H. Determination of preferred walking speed on treadmill may lead to high oxygen cost on treadmill walking. *Gait Posture* **31**, 366–369. https://doi.org/10.1016/j.gaitpost.2010.01.006 (2010).
52. Gaudreault, N., Gravel, D. & Nadeau, S. Evaluation of plantar flexion contracture contribution during the gait of children with Duchenne muscular dystrophy. *J. Electromyogr. Kinesiol.* **19**, e180–186. https://doi.org/10.1016/j.jelekin.2007.09.004 (2009).
53. Servais, L. et al. Evidentiary basis of the first regulatory qualification of a digital primary efficacy endpoint. *Sci. Rep.* **14**, 29681. https://doi.org/10.1038/s41598-024-80177-9 (2024).
54. Bach, M. M., Daffertshofer, A. & Dominici, N. Muscle synergies in children walking and running on a treadmill. *Front Hum. Neurosci.* **15**, 637157. https://doi.org/10.3389/fnhum.2021.637157 (2021).
55. Torricelli, F. et al. Motor invariants in action execution and perception. *Phys. Life Rev.* **44**, 13–47. https://doi.org/10.1016/j.plrev.2022.11.003 (2023).
56. Bleyenheuft, C. & Detrembleur, C. Kinematic covariation in pediatric, adult and elderly subjects: Is gait control influenced by age?. *Clin. Biomech.* **27**, 568–572. https://doi.org/10.1016/j.clinbiomech.2012.01.010 (2012).
57. Vandekerckhove, I. et al. Longitudinal interaction between muscle impairments and gait pathology in growing children with Duchenne muscular dystrophy. *J. Neuroeng. Rehabil.* **22**, 207. https://doi.org/10.1186/s12984-025-01718-5 (2025).
58. Ivanenko, Y. P., Cappellini, G., Dominici, N., Poppele, R. E. & Lacquaniti, F. Modular control of limb movements during human locomotion. *J. Neurosci.* **27**, 11149–11161. https://doi.org/10.1523/JNEUROSCI.2644-07.2007 (2007).
59. Aprigliano, F., Martelli, D., Micera, S. & Monaco, V. Intersegmental coordination elicited by unexpected multidirectional slipping-like perturbations resembles that adopted during steady locomotion. *J. Neurophysiol.* **115**, 728–740. https://doi.org/10.1152/jn.00327.2015 (2016).

60. Taga, G., Yamaguchi, Y. & Shimizu, H. Self-organized control of bipedal locomotion by neural oscillators in unpredictable environment. *Biol. Cybern.* **65**, 147–159. https://doi.org/10.1007/BF00198086 (1991).
61. Ivanenko, Y. P., d'Avella, A., Poppele, R. E. & Lacquaniti, F. On the origin of planar covariation of elevation angles during human locomotion. *J. Neurophysiol.* **99**, 1890–1898. https://doi.org/10.1152/jn.01308.2007 (2008).
62. Funato, T., Aoi, S., Tomita, N. & Tsuchiya, K. Validating the feedback control of intersegmental coordination by fluctuation analysis of disturbed walking. *Exp. Brain Res.* **233**, 1421–1432. https://doi.org/10.1007/s00221-015-4216-x (2015).
63. Hoellinger, T. et al. Biological oscillations for learning walking coordination: Dynamic recurrent neural network functionally models physiological central pattern generator. *Front. Comput. Neurosci.* **7**, 70. https://doi.org/10.3389/fncom.2013.00070 (2013).
64. Leurs, F. et al. Optimal walking speed following changes in limb geometry. *J. Exp. Biol.* **214**, 2276–2282. https://doi.org/10.1242/jeb.054452 (2011).
65. Dewolf, A. H., Meurisse, G. M., Schepens, B. & Willems, P. A. Effect of walking speed on the intersegmental coordination of lower-limb segments in elderly adults. *Gait Posture* **70**, 156–161. https://doi.org/10.1016/j.gaitpost.2019.03.001 (2019).
66. Desmedt, J. E. & Cheron, G. Somatosensory evoked potentials to finger stimulation in healthy octogenarians and in young adults: wave forms, scalp topography and transit times of parietal and frontal components. *Electroencephalogr. Clin. Neurophysiol.* **50**, 404–425. https://doi.org/10.1016/0013-4694(80)90007-3 (1980).
67. Doherty, T. J., Komori, T., Stashuk, D. W., Kassam, A. & Brown, W. F. Physiological properties of single thenar motor units in the F-response of younger and older adults. *Muscle Nerve* **17**, 860–872 (1994).
68. Stevens, J. C. & Choo, K. K. Spatial acuity of the body surface over the life span. *Somatosens. Mot. Res.* **13**, 153–166 (1996).
69. Goble, D. J. Proprioceptive acuity assessment via joint position matching: From basic science to general practice. *Phys. Ther.* **90**, 1176–1184. https://doi.org/10.2522/ptj.20090399 (2010).
70. Pratt, J., Chew, C.-M., Torres, A., Dilworth, P. & Pratt, G. Virtual model control: An intuitive approach for bipedal locomotion. *Int. J. Robot. Res.* **20**, 129–143. https://doi.org/10.1177/02783640122067309 (2001).
71. Nunez-Lisboa, M. et al. Understanding gait alterations: trunk flexion and its effects on walking neuromechanics. *J. Exp. Biol.* https://doi.org/10.1242/jeb.249307 (2024).
72. Preuschoft, H. Mechanical analyses of primate feet: II. The foot as a whole. *Z. Anat. Entwicklungsgesch.* **131**, 156–192 (1970).
73. Gebo, D. L. Plantigrady and foot adaptation in African apes: Implications for hominid origins. *Am. J. Phys. Anthropol.* **89**, 29–58 (1992).
74. Schmitt, D. & Larson, S. G. Heel contact as a function of substrate type and speed in primates. *Am. J. Phys. Anthropol.* **96**, 39–50 (1995).
75. Cunningham, C., Schilling, N., Anders, C. & Carrier, D. The influence of foot posture on the cost of transport in humans. *J. Exp. Biol.* **213**, 790–797 (2010).
76. Brown, T. G. The intrinsic factors in the act of progression in the mammal. In *Proceedings of the Royal Society of London. Series B, containing papers of a biological character* **84**, 308–319 (1911).
77. Pereira da Silva, J. D. et al. Altered release and uptake of gamma-aminobutyric acid in the cerebellum of dystrophin-deficient mice. *Neurochem. Int.* **118**, 105–114. https://doi.org/10.1016/j.neuint.2018.06.001 (2018).
78. Wu, W. C., Bradley, S. P., Christie, J. M. & Pugh, J. R. Mechanisms and consequences of cerebellar Purkinje cell disinhibition in a mouse model of Duchenne muscular dystrophy. *J. Neurosci.* **42**, 2103–2115. https://doi.org/10.1523/JNEUROSCI.1256-21.2022 (2022).
79. Prigogine, C. et al. Cerebellar dysfunction in the mdx mouse model of Duchenne muscular dystrophy: An electrophysiological and behavioural study. *Eur. J. Neurosci.* **60**, 6470–6489. https://doi.org/10.1111/ejn.16566 (2024).
80. Sbriccoli, A. et al. Architectural changes of the cortico-spinal system in the dystrophin defective mdx mouse. *Neurosci. Lett.* **200**, 53–56 (1995).
81. Carretta, D. et al. The organisation of spinal projecting brainstem neurons in an animal model of muscular dystrophy. A retrograde tracing study on mdx mutant mice. *Brain Res.* **895**, 213–222. https://doi.org/10.1016/s0006-8993(01)02108-4 (2001).
82. Tetorou, K., Aghaeipour, A., Singh, S., Morgan, J. E. & Muntoni, F. The role of dystrophin isoforms and interactors in the brain. *Brain* **148**, 1081–1098. https://doi.org/10.1093/brain/awae384 (2025).
83. Castro, A., Aguilar, J., Andres, C., Felix, R. & Delgado-Lezama, R. GABAA receptors mediate motoneuron tonic inhibition in the turtle spinal cord. *Neuroscience* **192**, 74–80. https://doi.org/10.1016/j.neuroscience.2011.06.073 (2011).
84. Mazzone, G. L., Mohammadshirazi, A., Aquino, J. B., Nistri, A. & Taccola, G. GABAergic mechanisms can redress the tilted balance between excitation and inhibition in damaged spinal networks. *Mol. Neurobiol.* **58**, 3769–3786. https://doi.org/10.1007/s12035-021-02370-5 (2021).

85. Mizuno, Y., Yoshida, M., Yamamoto, H., Hirai, S. & Ozawa, E. Distribution of dystrophin isoforms and dystrophin-associated proteins 43DAG (A3a) and 50DAG (A2) in various monkey tissues. *J. Biochem.* **114**, 936–941. https://doi.org/10.1093/oxfordjournals.jbchem.a124281 (1993).
86. Zarrouki, F. et al. Abnormal expression of synaptic and extrasynaptic GABA(A) receptor subunits in the dystrophin-deficient mdx mouse. *Int. J. Mol. Sci.* https://doi.org/10.3390/ijms232012617 (2022).

Publisher's note Springer Nature remains neutral with regard to jurisdictional claims in published maps and institutional affiliations.

Authors and Affiliations

Ruiz Pablo[1] · Cheron Guy[1] · Deconinck Nicolas[1,2] · Cebolla Ana Maria[1]

✉ Cebolla Ana Maria
ana.maria.cebolla.alvarez@ulb.be

[1] NeuroMove, Laboratory of Movement Neurophysiology, Université Libre de Bruxelles, Brussels, Belgium

[2] Department of Pediatric Neurology and Neuromuscular Reference Center, Hôpital Universitaire des Enfants Reine Fabiola (HUB), Université Libre de Bruxelles, Brussels, Belgium